Electronic Supplementary Material (ESI) for Polymer Chemistry.

Supporting Information for:

Highly-ordered onion micelles made from amphiphilic highly-branched copolymers

Sarah L. Canning, Joseph M. F. Ferner, Natalie M. Mangham, Trevor J. Wear, Stuart W. Reynolds, Jonathan Morgan, J. Patrick A. Fairclough, Stephen M. King, Tom Swift, Mark Geoghegan, and Stephen Rimmer

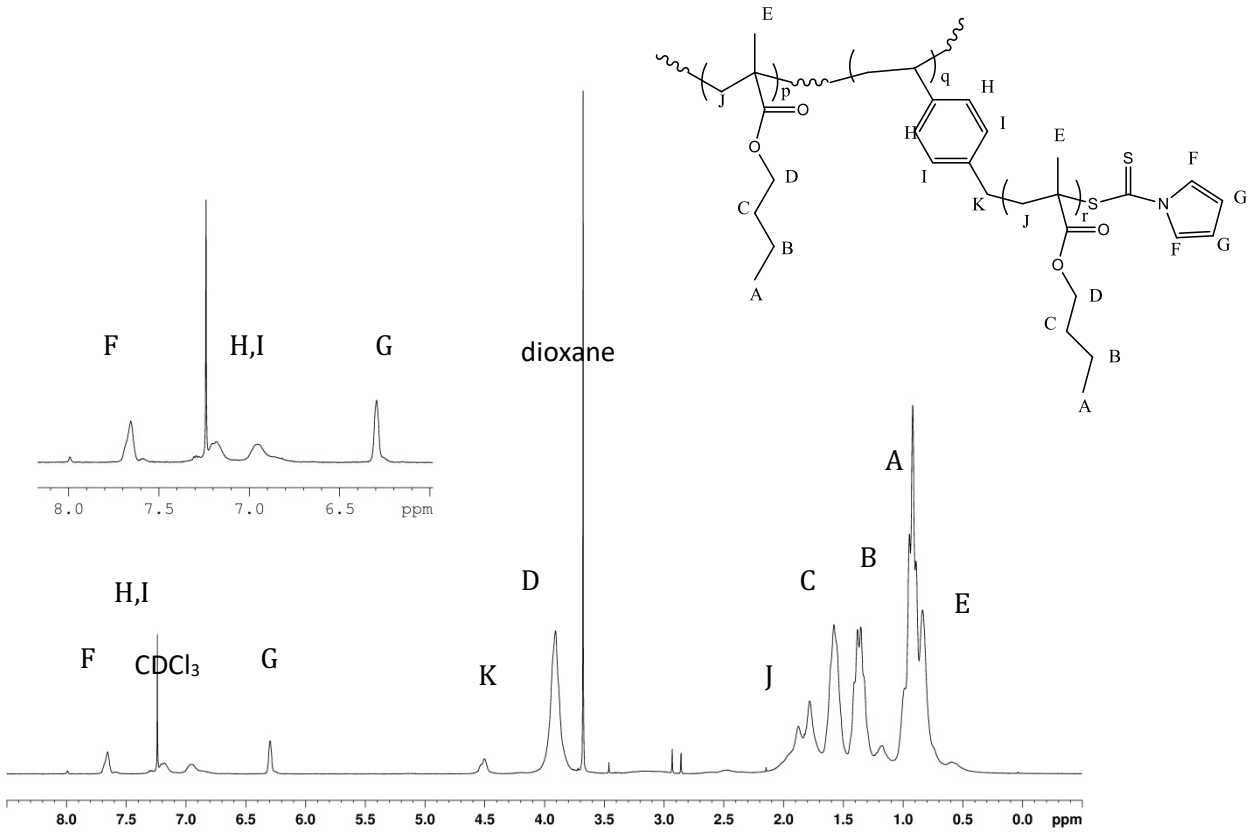

Figure S1 Assigned 1H NMR spectrum of HB-PBMA macro-CTA in $CDCl_3$, with the expanded region showing the peaks due to the pyrrole groups (F and G) and styryl groups (H and I) originating from the CTA

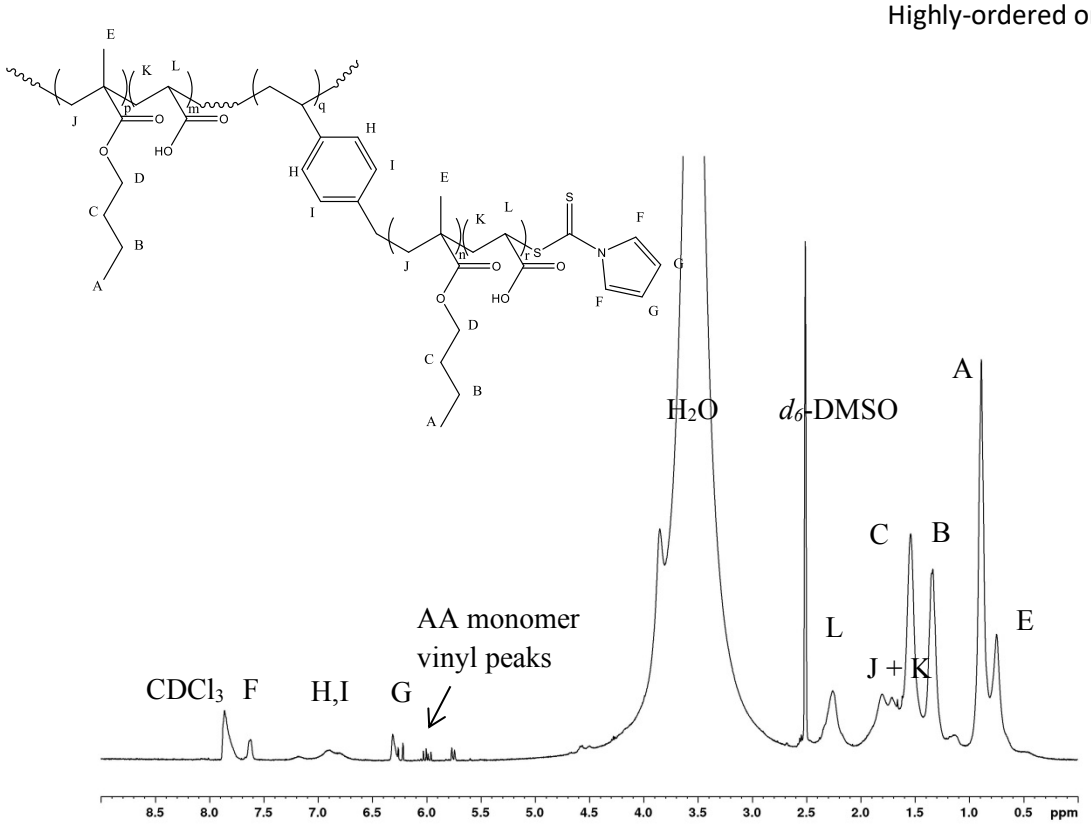

Figure S2 Assigned 1H NMR spectrum of HB-PBMA$_{1.4}$-PAA$_{1.0}$ in 1:1 $CDCl_3$:d_6-DMSO

Characterization details for:

4-Vinylbenzyl-1-pyrrolecarbodithioate

R_f (silica, hexane): 0.14.

1H NMR ($CDCl_3$, 250 MHz) δ/ppm: 4.60 (s, 1H, -C(=S)-S-C**H**$_2$-), 5.28 (d, J = 10.93 Hz, 1H, -CH=C**H**H), 5.76 (d, J = 17.60 Hz, 1H, -CH=CH**H**), 6.34 (t, J = 2.43 Hz, 2H, Ar), 6.71 (dd, J = 17.60, 10.88 Hz, 1H, -C**H**=CH$_2$), 7.38 (m, 4H, Ar), 7.72 (t, J = 2.37 Hz, 2H, Ar)

13C NMR ($CDCl_3$, 63 MHz) δ/ppm: 40.94 (1C, -C(=S)-S-**C**H$_2$**-),** 113.69 (2C, Ar), 113.83 (1C, **C**H$_2$=CH-), 120.10 (2C, Ar), 126.00 (2C, Ar), 129.06 (2C, Ar), 133.96 (1C, Ar), 135.65 (1C, -**C**H=CH$_2$) , 199.27 (1C, -**C(**=S)S-)

Calculated for $C_{14}H_{13}NS_2$: C, 64.83; H, 5.05; N, 5.40; S, 24.72. Found: C, 64.35; H, 5.13; N, 4.99; S, 22.50.

EI MS m/z: 259 (calculated 259)

HB PMMA

1H NMR ($CDCl_3$, 400 MHz) δ/ppm: 0.95 (d, J= 69.43 Hz, 3H, -CH$_3$), 1.90 (br, 2H, -C**H**$_2$C(CH$_3$)(C(=O)OC**H**$_3$), 3.62 (br, 2H, C(=O)OCH$_3$), 6.36 (m, 2H, Ar), 7.17-7.44 (br, 4H, Ar), 7.69 (br, 2H, Ar)

HB PBMA

1H NMR ($CDCl_3$, 400 MHz) δ/ppm: : 0.89 (s, 3H, -CH_3), 1.00 (br, 3H, -$(CH_2)_3C\mathbf{H}_3$), 1.42 (br, 2H, -$(C\mathbf{H}_2)CH_3$), 1.62 (br, 2H, -$(C\mathbf{H}_2CH_2CH_3$), 1.92 (br, 2H, -$C\mathbf{H}_2C(CH_3)(C(=O)O(CH_2)_3CH_3$-), 3.96 (br, 2H, C(=O)O$C\mathbf{H}_2$-), 4.63 (br, 1H, C**H**Ar), 6.34 (m, 2H, Ar), 7.30-7.45 (br, 4H, Ar), 7.72 (br, 2H, Ar)

HB PLMA

1H NMR ($CDCl_3$, 400 MHz) δ/ppm: 0.91 (br, 3H, -CH_3), 1.00 (br, 3H, -$(CH_2)_{11}C\mathbf{H}_3$), 1.42 (br, 18H, -$(C\mathbf{H}_2)_9CH_3$), 1.62 (br, 2H, -$(C\mathbf{H}_2(CH_2)_9CH_3$), 1.92 (br, 2H, -$C\mathbf{H}_2C(CH_3)(C(=O)O(CH_2)_{11}CH_3$), 3.94 (br, 2H, C(=O)O$C\mathbf{H}_2$-), 6.37 (m, 2H, Ar), 7.30-7.45 (br, 4H, Ar), 7.67 (br, 2H, Ar)

HB-PMMA-PAA

1H NMR (1:1 $CDCl_3$:DMSO-d_6 , 400 MHz) δ/ppm: 0.94-0.66 (br, 3H, -CH_3), 1.32-0.95 (br, 2H, -$C\mathbf{H}_2C(CH_3)(C(=O)OCH_3$), 1.86 (br, 2H, -$C\mathbf{H}_2$CHCOOH), 3.52 (br, 2H, C(=O)O$C\mathbf{H}_3$), 4.57 (br, 2H, -$C\mathbf{H}_2$Ar-), 6.34 (br, 2H, Ar), 7.30-7.45 (br, 4H, Ar), 7.67 (br, 2H, Ar), 11.87 (s, 1H, -COO**H**)

13C NMR (1:1 $CDCl_3$:DMSO-d_6 , 100 MHz) δ/ppm: 22.78 (1C, -$\mathbf{C}H_3$), 44.40 (1C, -$\mathbf{C}$HC(**=**O)OH), 51.84 (1C, -C(=O)OCH_3), 176.37 (1C, -$\mathbf{C}$(=O)OH), 177.47 (1C, -$\mathbf{C}$(=O)OCH_3)

HB-PBMA$_{1.4}$-PAA$_{1.0}$

1H NMR (1:1 $CDCl_3$:DMSO-d_6 , 400 MHz) δ/ppm: 0.89 (s, 3H, -CH_3), 1.00 (br, 3H, -$(CH_2)_3C\mathbf{H}_3$), 1.42 (br, 2H, -$(C\mathbf{H}_2)CH_3$), 1.62 (br, 2H, -$(C\mathbf{H}_2CH_2CH_3$), 1.92 (br, 4H, -$C\mathbf{H}_2C(CH_3)(C(=O)O(CH_2)_3CH_3$- and -$C\mathbf{H}_2$CHCOOH), 3.96 (br, 2H, C(=O)O$C\mathbf{H}_2$-), 2.22 (s, 1H, CHCOOH), 4.57 (br, 2H, -$C\mathbf{H}_2$Ar-), 6.34 (br, 2H, Ar), 7.30-7.45 (br,
4H, Ar), 7.67 (br, 2H, Ar), 11.96 (s, 1H, -COO**H**)
250

13C NMR (1:1 $CDCl_3$:DMSO-d_6 , 100 MHz) δ/ppm: 13.75 (1C, -$(CH_2)_3\mathbf{C}H_3$), 19.28 (1C, -$(CH2)_2\mathbf{C}H_2CH_3$), 30.16 (1C, -$CH_2\mathbf{C}H_2CH_2CH_3$), 44.60 (1C, -$\mathbf{C}$HC(=O)OH), 64.58 (1C, -C(=O)O$\mathbf{C}H_2$-), 176.37 (1C, -$\mathbf{C}$(=O)OH), 177.52 (1C, -$\mathbf{C}$(=O)O$(CH_2)_3CH_3$)

HB-PLMA-PAA

1H NMR (1:1 $CDCl_3$:DMSO-d_6 , 400 MHz) δ/ppm: 0.91 (br, 3H, -CH_3), 1.00 (br, 3H, -$(CH_2)_{11}C\mathbf{H}_3$), 1.42 (br, 18H, -$(C\mathbf{H}_2)_9CH_3$), 1.62 (br, 2H, -$(C\mathbf{H}_2(CH_2)_9CH_3$), 1.92 (br, 2H, -$C\mathbf{H}_2C(CH_3)(C(=O)O(CH_2)_{11}CH_3$ and -$C\mathbf{H}_2$CHCOOH), 3.94 (br, 2H, C(=O)O$C\mathbf{H}_2$-), 4.59 (br, 2H, -$C\mathbf{H}_2$Ar-), 6.34 (br, 2H, Ar), 7.30-7.45 (br, 4H, Ar), 7.67 (br, 2H, Ar), 11.94 (s, 1H, -COO**H**)

13C NMR (1:1 $CDCl_3$:DMSO-d_6 , 100 MHz) δ/ppm: 14.18 (1C, -$(CH_2)_{11}\mathbf{C}H_3$), 22.62

(1C, -$(CH_2)_{10}$**C**H_2CH_3), 29.29 (3C, -$(CH_2)_6$(**C**H_2)$_3$$(CH_2)_2CH_3$), 29.61 (5C, -CH2(**C**$H_2$)$_5$$(CH_2)_5CH_3$), 31.87 (1C, -**C**$H_2CH_2CH_3$), 64.69 (1C, -C(=O)O**C**H_2-), 176.28 (1C, -**C**(=O)OH), 177.41 (1C, -**C**(=O)O$(CH_2)_{11}CH_3$)

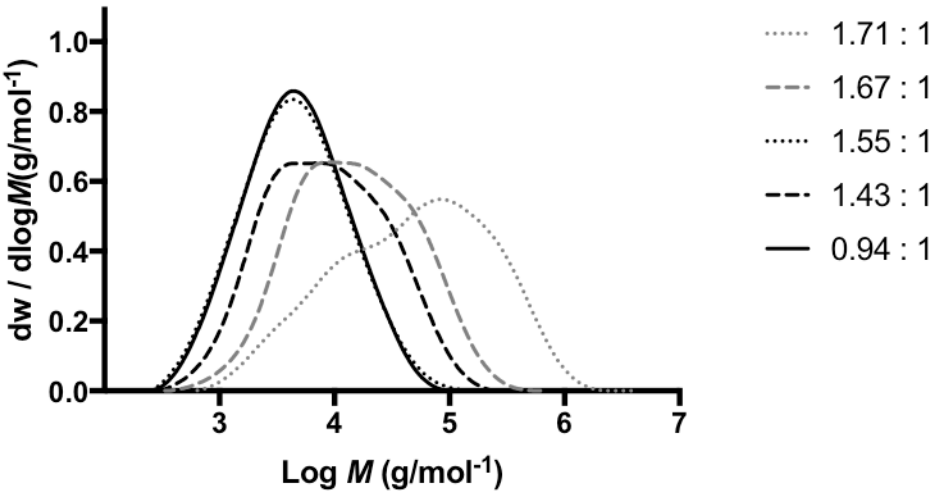

Figure S3 Molar mass distribution from GPC of non-onion forming HB-PBMA-PAA formulations

Effect of rate of water addition on self-assembly

Several experiments were carried out to aid in determining the mechanism of onion micelle formation. The first of these was the investigation of the effect of the rate of block-selective solvent addition to the copolymer solution. Five different rates of water addition were selected and the resulting dispersions analyzed; however, it was concluded from statistical analysis of the data that the rate of water addition did not control the structure of the onion micelles.

The effect of the rate of block-selective solvent addition to the copolymer solution was investigated. The water was added using a syringe pump to ensure a constant addition rate, which meant that the rate could be easily varied. Five different water addition rates were selected: 0.05, 0.10, 0.20, 0.50 and 1.00 ml min^{-1}, and dispersions prepared at each rate were analysed by TEM and PALS. **Figure S4** shows example TEM images of onion micelles prepared at each addition rate. The diameters of the onion lamellae were measured using ImageJ image analysis software and are represented graphically in **Figure S5**.

A one-way ANOVA with Tukey post-hoc analysis was carried out on these data to determine whether there are statistically significant differences between the means of the different addition rates. These are indicated on the graph in **Figure S5**. However, it was concluded from statistical analysis of the data that the rate of water addition did not control the structure of the onion micelles.

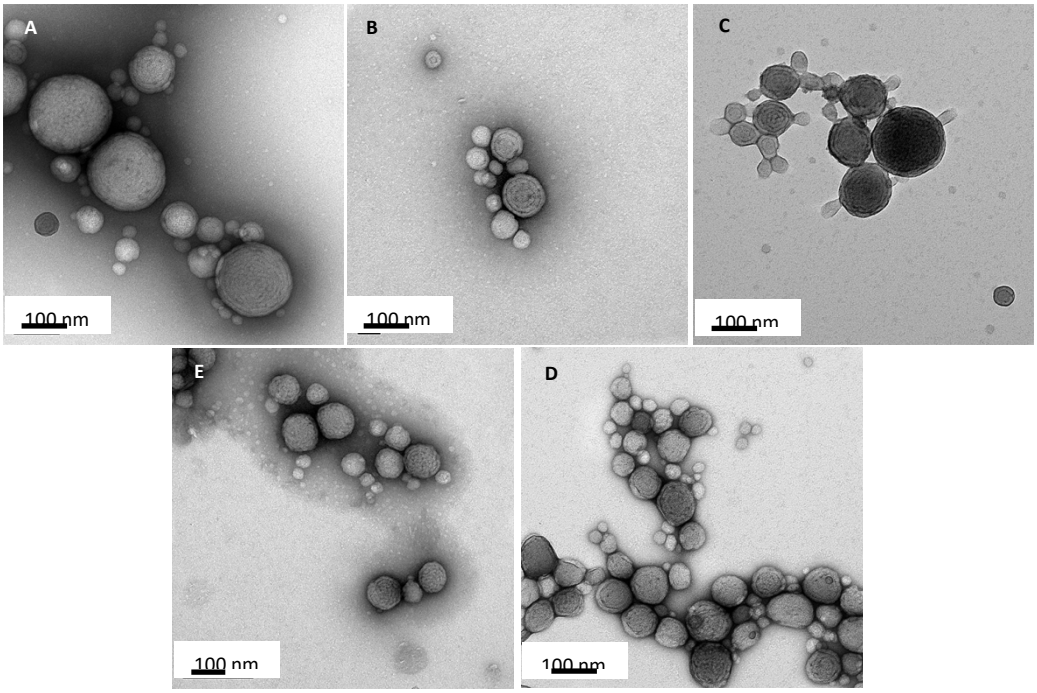

Figure S4. Representative TEM images of HB-PBMA$_{1.4}$-PAA$_{1.0}$ self-assembled in water at different rates of water addition: A) 0.05, B) 0.10, C) 0.20, D) 0.50 and E) 1.00 ml min^{-1}. Samples are stained with uranyl formate. Lamellar structure is observed in each image

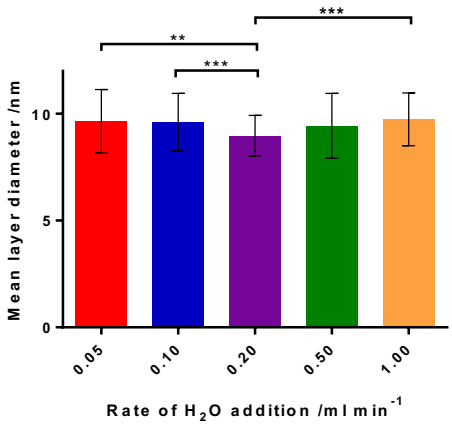

Figure S5. Graph of mean layer diameter of onion micelles, as calculated from TEM images using ImageJ software, at different rates of water addition to HB-PBMA$_{1.4}$-PAA$_{1.0}$ solution in THF. Error bars represent standard deviation. Tie lines show significance level of comparisons between sets of copolymers: *** P<0.001, ** 0.001<P<0.01, * 0.01<P<0.5, ns (not significant) P ≥ 0.05. Here, only significant relationships between copolymers are shown on the graph

UV-vis absorption spectroscopy

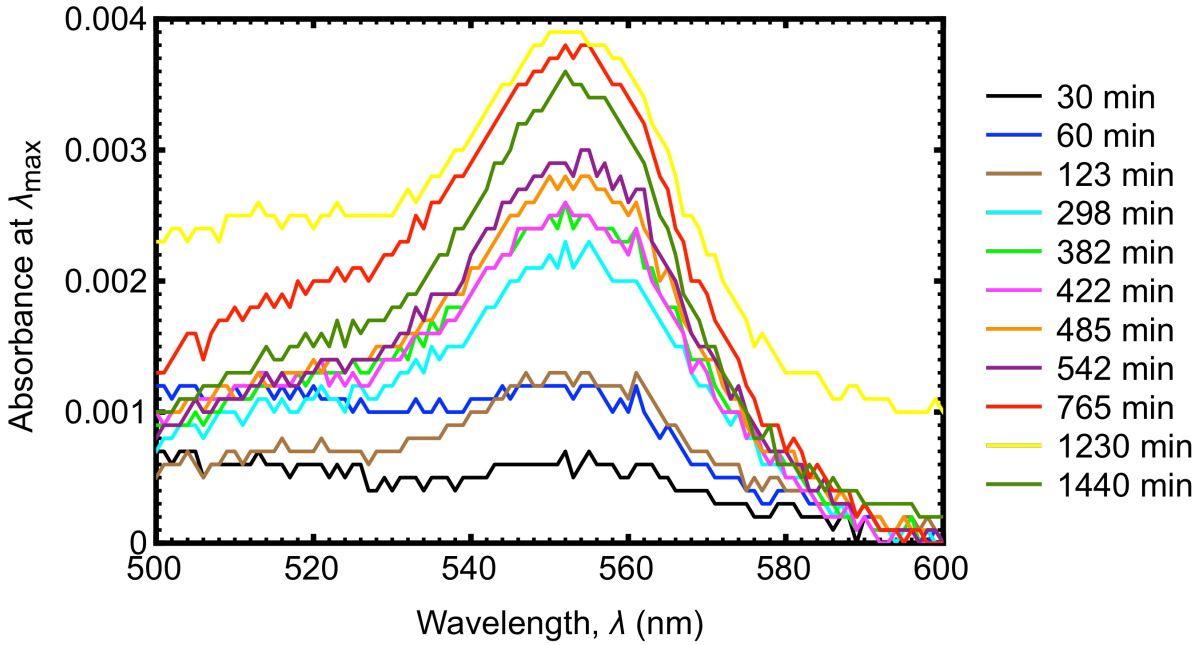

Figure S6. UV-vis absorption data (above) were obtained as a function of time to test for rhodamine B release from an aqueous HB-PBMA$_{1.4}$-PAA$_{1.0}$ preparation during heating at 45 °C. Two sets of experiments were performed (of which the above data represent one) and the average was taken to obtain the release profile shown in Figure 10

Lamellar paracrystal model

$$I(Q) = 2\pi(\Delta\rho)^2 \Gamma_m \frac{P_{bil}(Q)}{Q^2} Z_N(Q) \qquad \textbf{(S1)}$$

$$P_{bil}(Q) = \left(\frac{\sin(Qt/2)}{(Qt/2)}\right)^2 \qquad \textbf{(S2)}$$

$$N_L = x_N N + (1 - x_N)(N + 1) \qquad \textbf{(S3)}$$

Equation S1 is used to calculate the scattering, where $\Delta\rho$ represents the difference in scattering length density between the solvent and the polymer (the contrast), $Z_N(Q)$ represents the interference effects where more than one bilayer is present and Γ_m is the mass per area of the bilayer. In this application of the model, the scale factor is used instead of Γ_m and represents the volume fraction of the material forming the bilayer. $P_{bil}(Q)$ is the form factor of the bilayer, given by **Equation S2** in which it is approximated as the cross section of an infinite planar bilayer, where t represents the layer thickness. Where there is a non-integer number of layers (N_L), **Equation S3** is used to calculate the value from a linear combination of the higher and lower values.

Additional TEM images

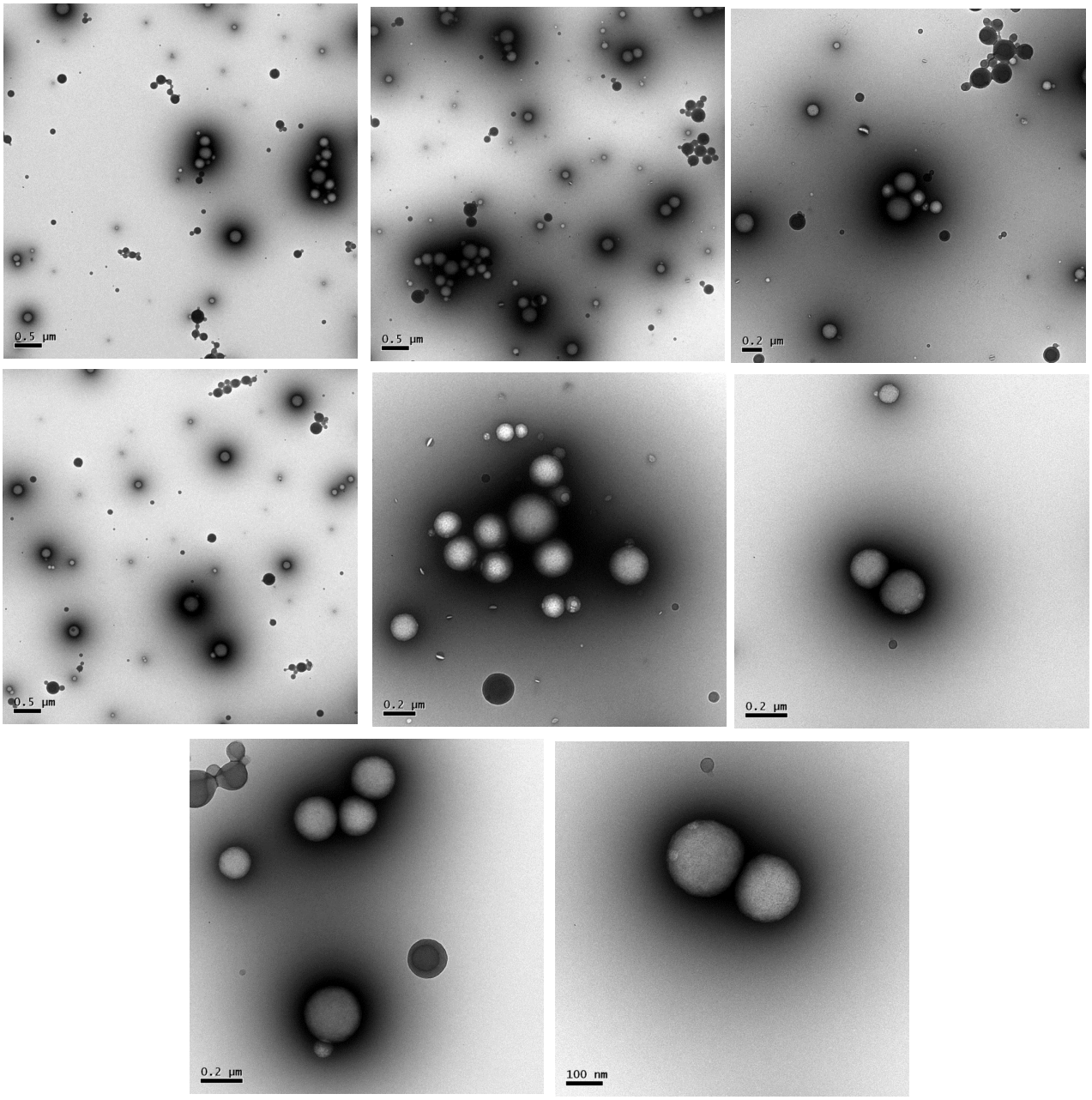

Figure S7. TEM micrographs of dispersions of HB-PMMA-PAA in water, stained with uranyl formate. These supplement Figure 2A

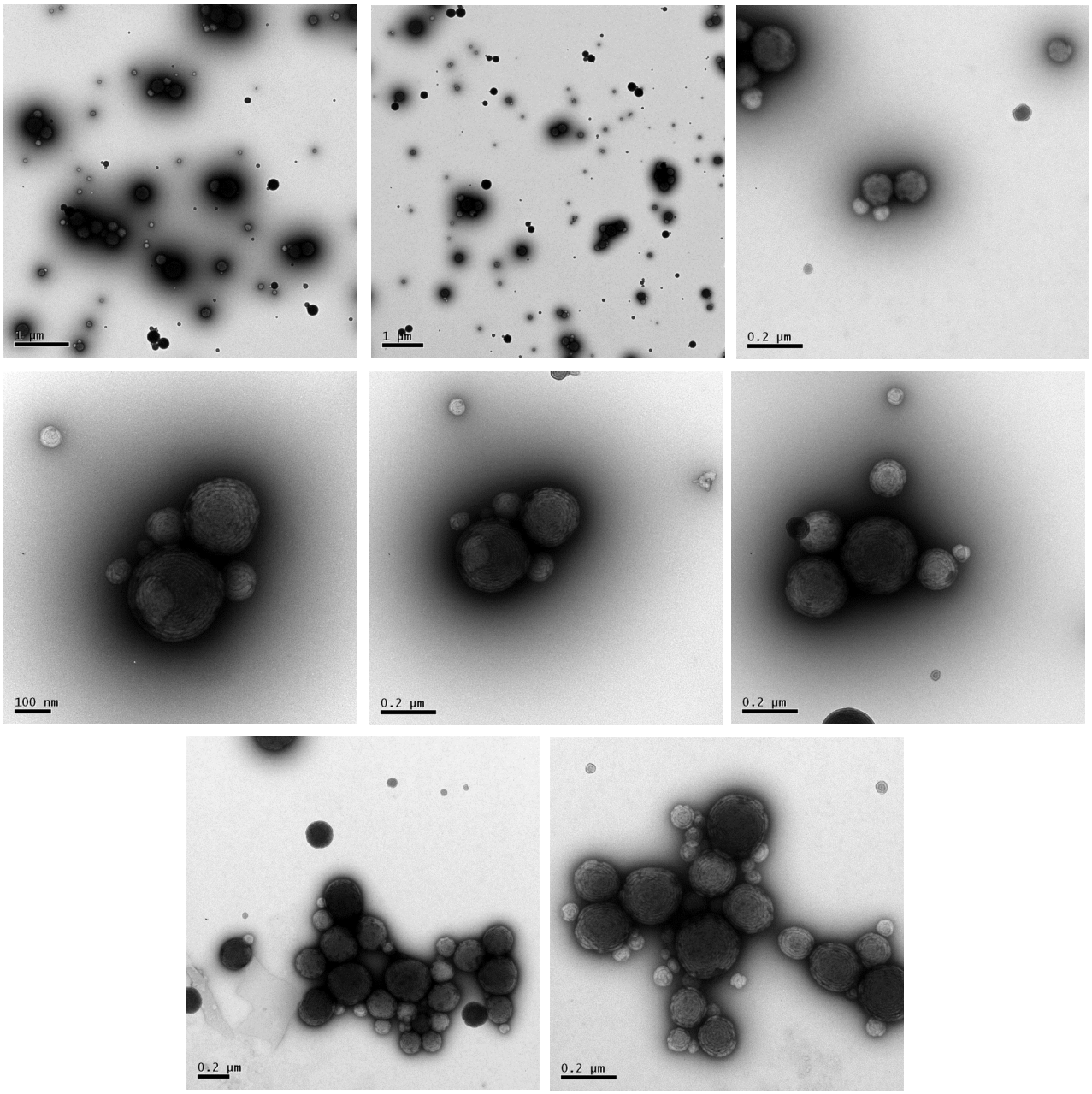

Figure S8. TEM micrographs of dispersions of HB-PBMA$_{1.4}$-PAA$_{1.0}$ in water, stained with uranyl formate. These supplement Figure 2B

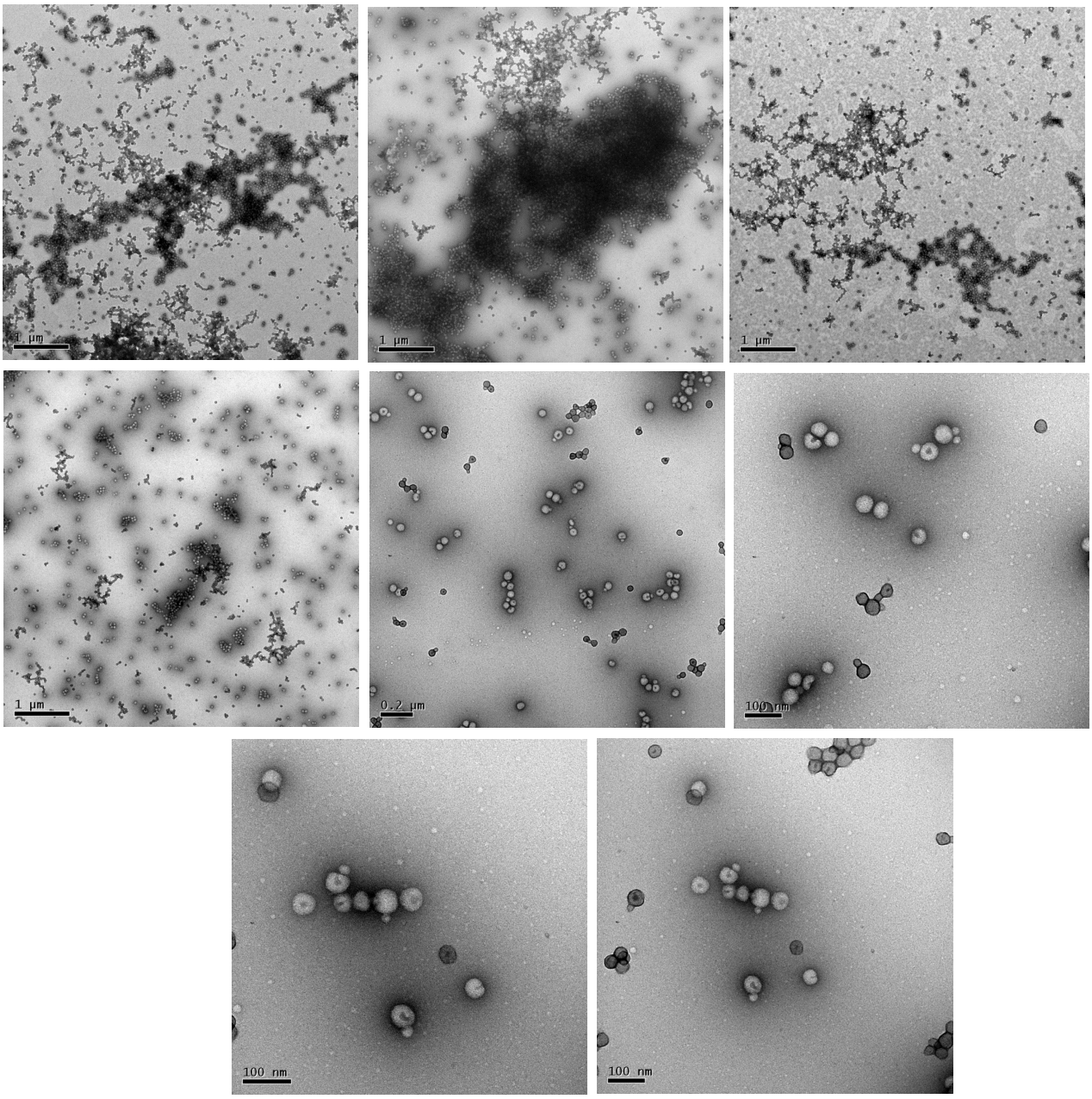

Figure S9. TEM micrographs of dispersions of HB-PLMA-PAA in water, stained with uranyl formate. These supplement Figure 2C

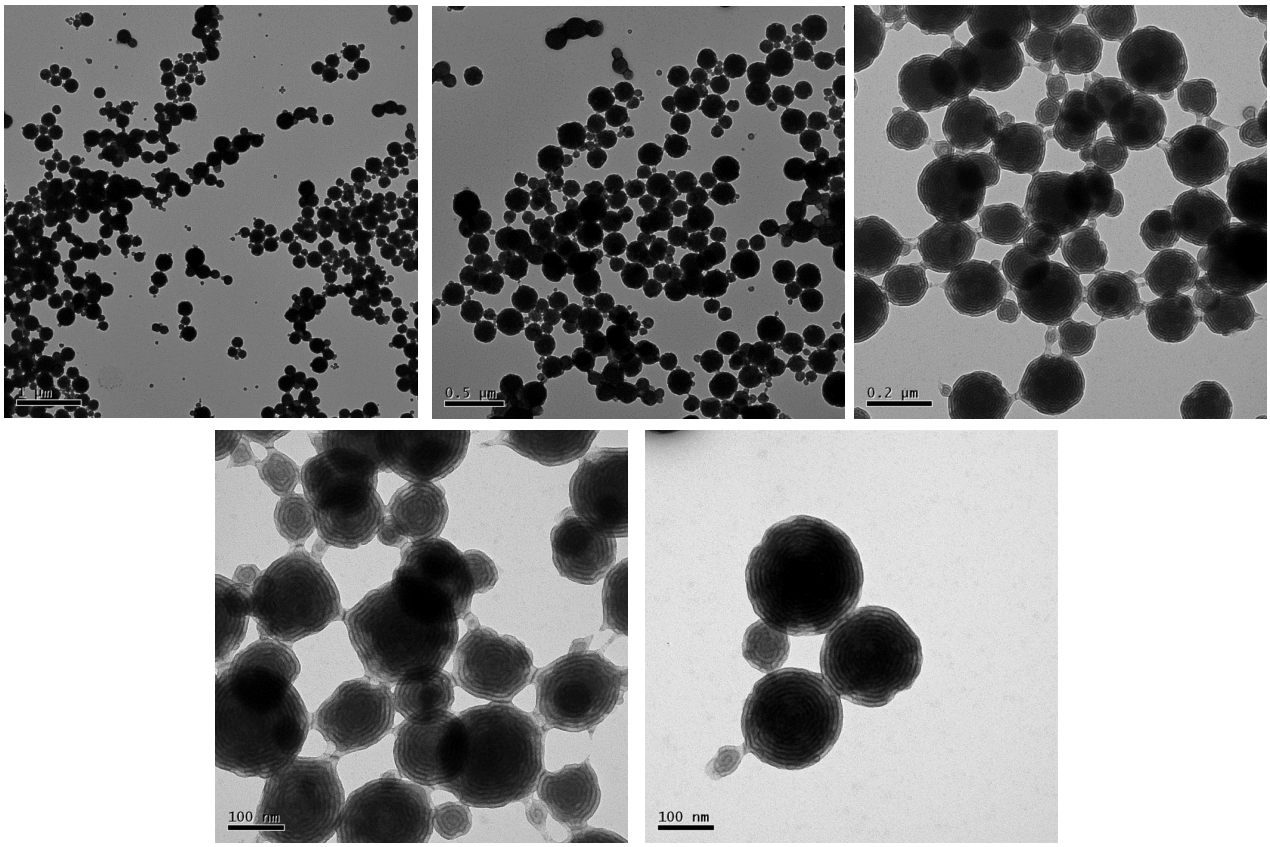

Figure S10. TEM images of onion micelles formed from HB-PBMA$_{1.4}$-PAA$_{1.0}$ dispersed in water after 5 weeks storage at ambient conditions. These images supplement Figure 5C and 5D

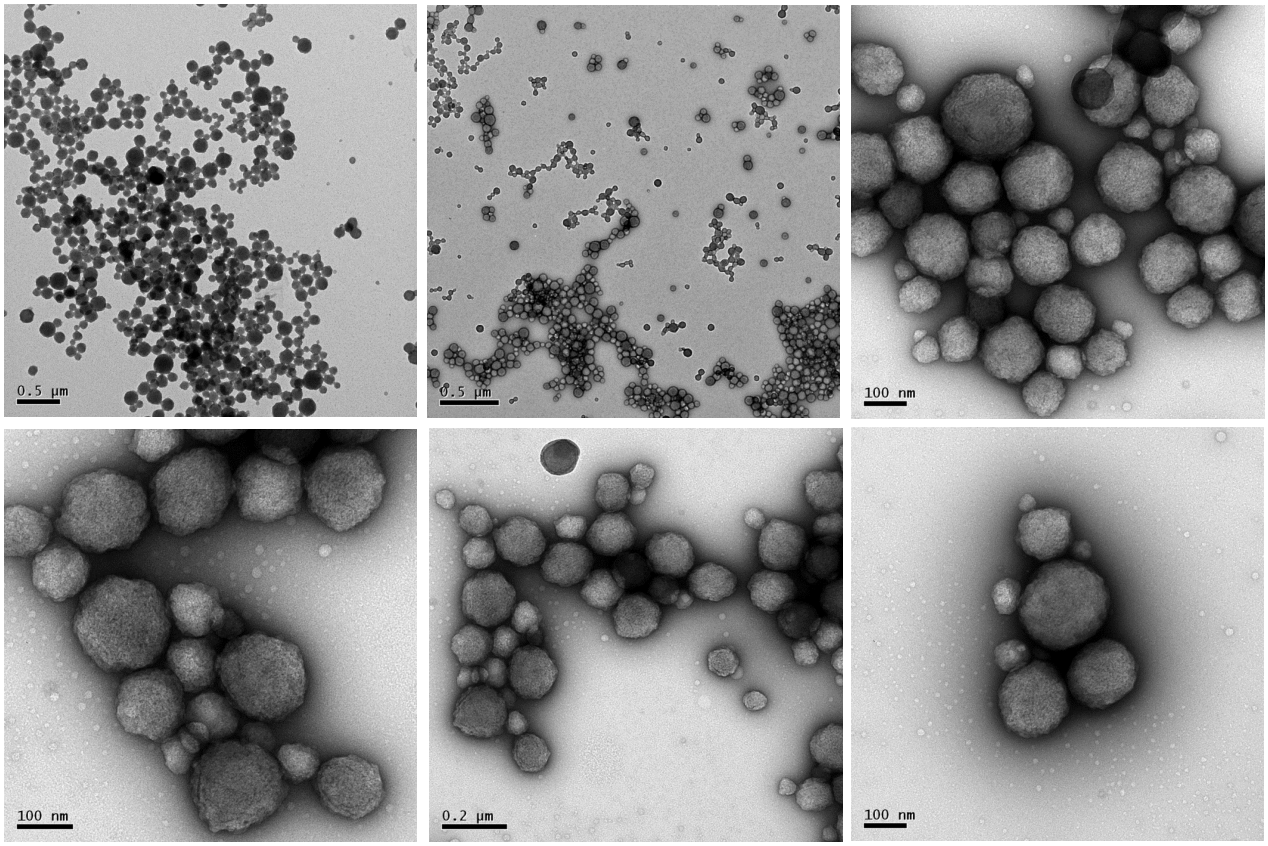

Figure S11. Representative TEM images of HB-PMMA-PAA following annealing at 45°C for 12 h. Samples were stained with uranyl formate prior to imaging. These images supplement Figure 6D

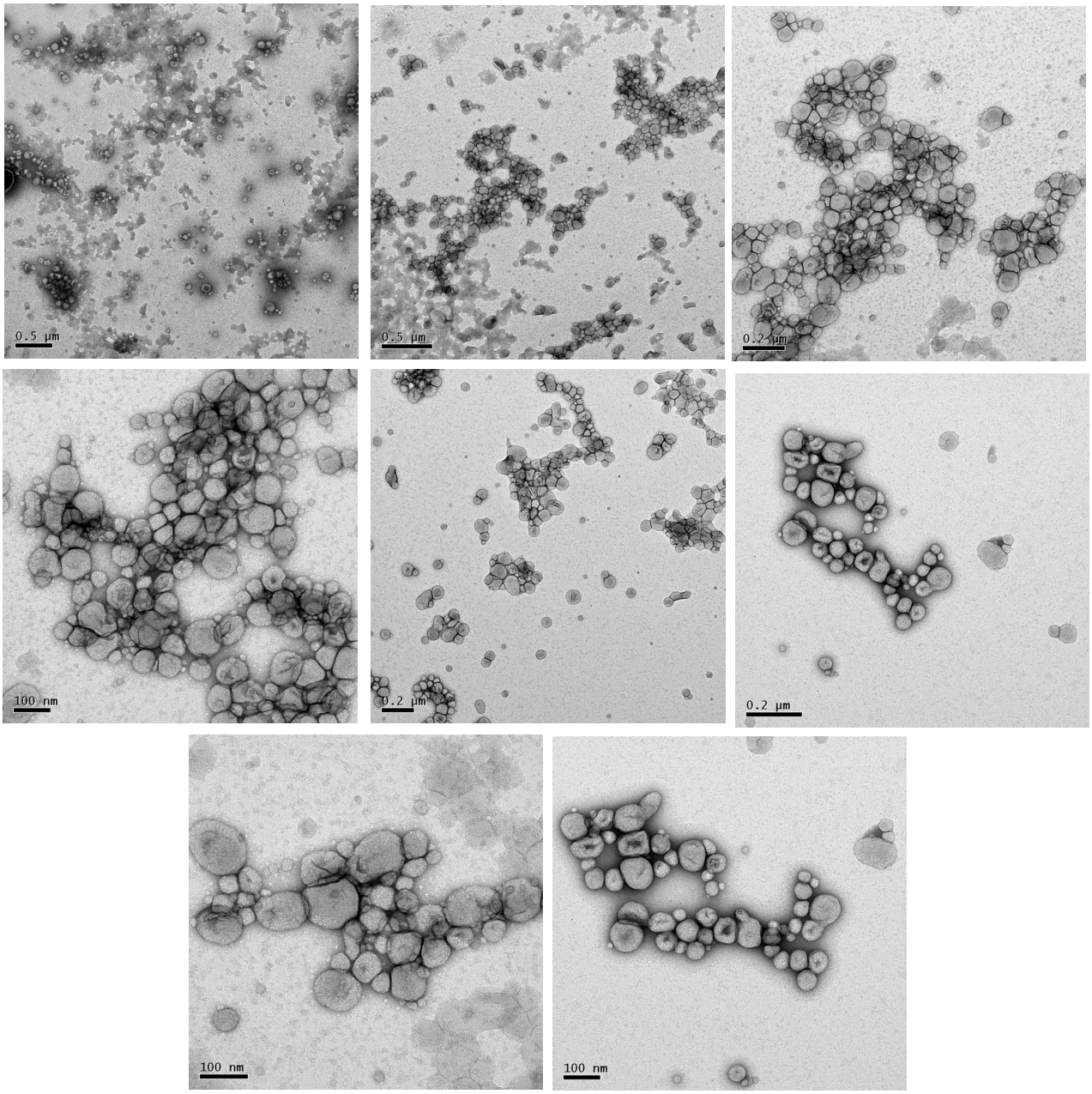

Figure S12. Representative TEM images of HB-PBMA$_{1.4}$-PAA$_{1.0}$ following 12 h annealing at 45°C. The samples were stained with uranyl formate. These images supplement Figure 6E

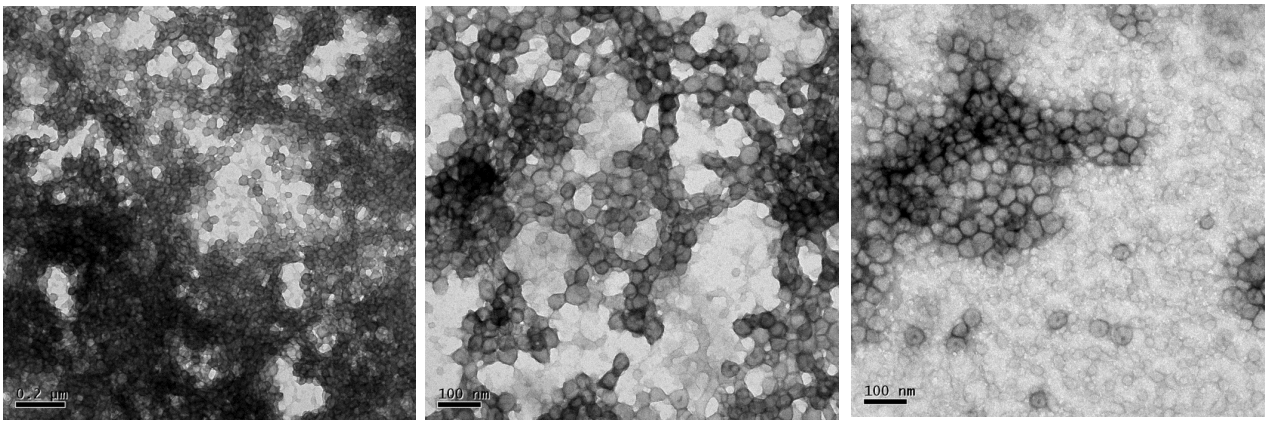

Figure S13. Representative TEM images of HB-PLMA-PAA following annealing at 45°C for 12 h. The samples were stained with uranyl formate. These images supplement Figure 6F

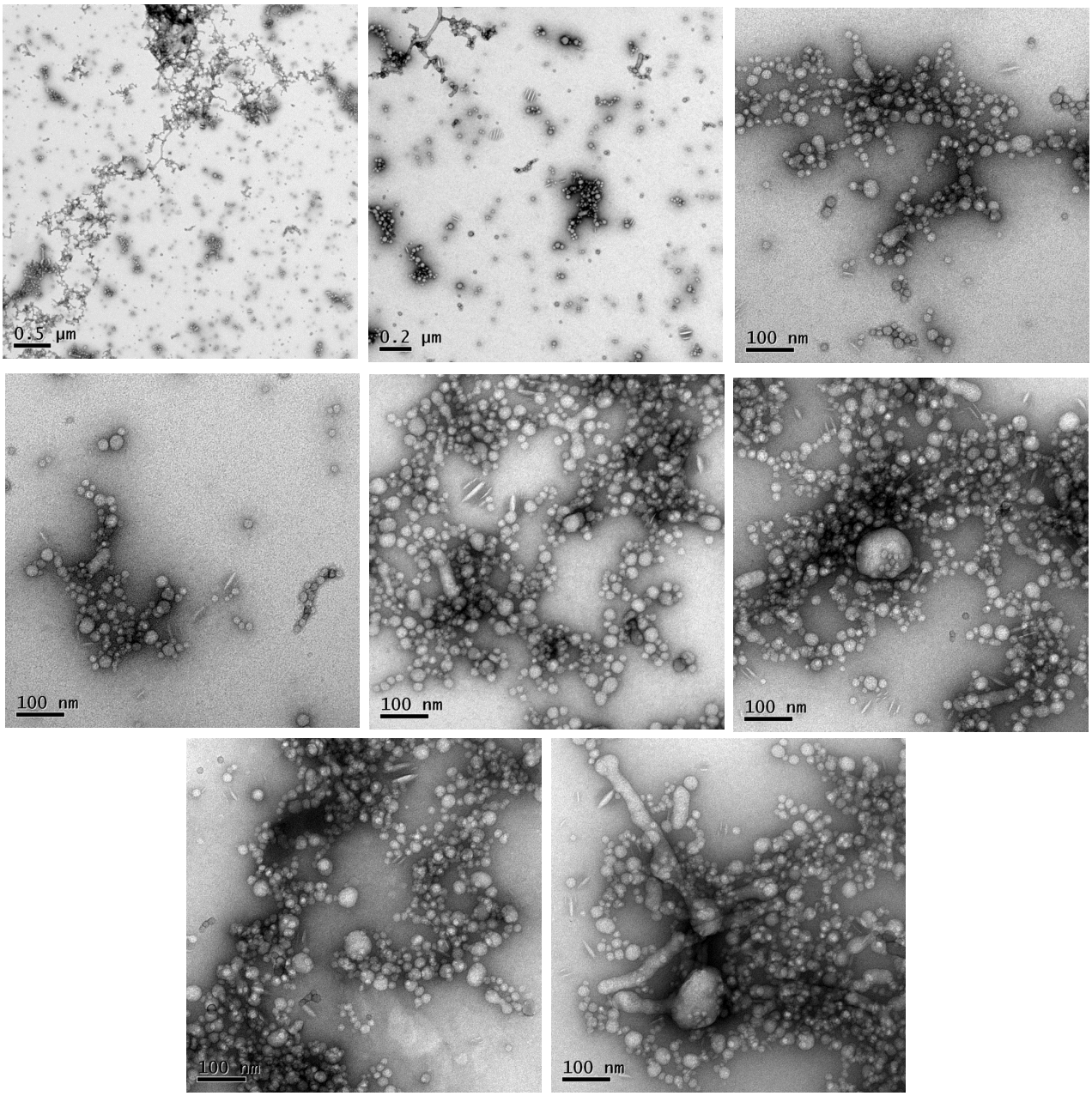

Figure S14. Representative TEM images of HB-PBMA$_{1.4}$-PAA$_{1.0}$ copolymer self-assembled in water. Following water addition, samples were dialyzed against water for 24 hours to remove residual THF, instead of the evaporation step. Samples were stained with uranyl formate prior to imaging. Predominantly small spherical micelles are observed, with some evidence of coalescence into worm-like structures. These images supplement Figure 7